j = plate number; $j = 0$ denotes the hot end of the unit

J = number of the plate at the cool end of the unit

p = feed stream number; $p = 1$ denotes the feed nearest the hot end of the unit

P = number of the feed nearest the cool end of the unit; this is the total number of feeds to the unit

s = side-draw number; $s = 1$ denotes the side draw nearest the hot end of the unit

S = number of the side draw nearest the cool end of the unit; this is the total number of side draws

LITERATURE CITED

1. Ball, W. E., paper presented at A.I.Ch.E. New Orleans meeting (Feb. 27, 1961).
2. Bloeman, Ir. F., *Rev. Franc. Corps Gras*, **6**, 90-103 (1959).
3. Friday, J. R., and B. D. Smith, *A.I.Ch.E. J.*, **10**, No. 5, 698-707 (1964).
4. Holland, C. D., "Multicomponent Distillation," Prentice-Hall, Englewood Cliffs, N. J. (1963).
5. Kern, D. Q., and Wm. Van Nostrand, *Ind. Eng. Chem.*, **41**, 2209-12 (1949).
6. Markley, Klare S., "Fatty Acids," Interscience, New York (1947).
7. Peaceman, D. W., and H. H. Rachford, Jr., *J. Soc. Ind. Appl. Math.*, **3**, 28-65 (1955).
8. Pool, W. O., and A. W. Ralston, *Ind. Eng. Chem.*, **34**, 1104-5 (1942).
9. Rall, L. B., ed., "Error in Digital Computation," Vol. 1, Wiley, New York (1965).

APPENDIX

1. Double subscripts or subscripted subscripts are written as compound subscripts. Thus, $v_{w,j+1}$ becomes v_{wj+1} and l_{j_s-1} becomes l_{js-1}. l_{j_s-1} does not occur
2. Σ without indices denotes a sum over all components at plate j
3. $\tilde{\Sigma}$ without indices denotes a sum over one component or quantity entering or leaving the unit from the hot end to and including plate j
4. Δ denotes that the quantity on one side is defined as equal $\overset{=}{}$ to the quantity on the other

Manuscript received September 30, 1965; revision received March 31, 1966; paper accepted April 15, 1966.

Reverse Osmosis in Annuli

WILLIAM N. GILL

Clarkson College of Technology, Potsdam, New York

DALE W. ZEH and CHI TIEN

Syracuse University, Syracuse, New York

The nonlinear problem of reverse osmosis in annular conduits is solved by a series expansion method which is very accurate in the diffusion entrance region near the inlet of the membrane section. It is found that polarization at the outer membrane surface is significantly greater than at the inner wall.

In the diffusion entrance region, for the problem considered, the degree of polarization depends on the three parameters σ, η_k, and B_2, which are known once the operating conditions and the physical properties of the system are specified. The quantities θ_i (0) are tabulated for a wide range of η_k and B_2. With these quantities known one can apply Equation (17) at $\beta = 0$ to calculate the wall concentration distribution and, with Equation (4), the flux distribution along the system. Then, by using Equation (26), the water produced by the system can be determined explicitly in terms of prescribed operating conditions.

Reverse osmosis is currently being studied from various points of view because of its potential as a process for sea and brackish water desalination. Interest in reverse osmosis was sparked by the report of Bretton and Reid (*1*) in 1957 that cellulose acetate films yielded salt rejection of 97 to 98% at an operating pressure of 850 lb./sq.in. with a throughput of some 0.15 gal./(sq.ft.)(day). This membrane was improved very substantially by Loeb (5) to the point where water fluxes up to 20 gal./(sq.ft.)(day) are currently feasible.

Basic research in reverse osmosis is directed along at least two lines. For obvious reasons, there is considerable interest in developing a better understanding of the fundamental transport processes which occur within the membrane structure. Another area of interest relates to the nonlinear diffusional effects on the brine side of the system. A good discussion of the kinetics of water and salt transport in cellulose acetate membranes was given very recently by Michaels, Bixler, and Hodges (7). Several discussions of brine side diffusional effects, concentration polarization in particular, are available (*2* to *4*, *6*, *8*, *9*). Sherwood, Brian, Fisher, and Dresner (*8*) studied the linear problem of constant water flux along the membrane in fully developed flow between parallel plates. Gill, Tien, and Zeh (2) considered the nonlinear problem wherein the salt concentration at the membrane surface increases along the direction of flow, and therefore the water flux through the membrane decreases with axial distance. Since the Schmidt number for salt water is about 560, the diffusion boundary layer is much thinner than the momentum boundary layer, and, therefore, the velocity components can be represented by expressions which are accurate only in the region near the wall. The method of analysis which will be employed here does not require

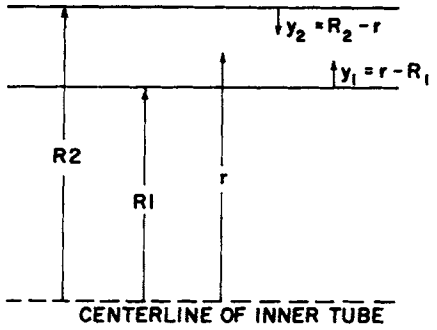

Fig. 1. Coordinate system.

the use of this assumption, but it does simplify the problem somewhat.

A variety of geometries may very well be used for reverse osmosis systems, and it is quite possible that such geometries will have transverse curvature. Thus, the present work investigates reverse osmosis in annuli so that as a special case, the diffusion inlet region of a tube is included. Indeed, tubular membrane channels have been developed and tested (*10, 11*).

Fisher, Sherwood, and Brian (9) studied a diffusion problem in tubes wherein they assumed that the water flux through the tubular membrane surface is constant along the direction of flow. This is a limiting case for reverse osmosis and would be exact if the operating pressure were infinite. In the present work we relax the assumption of constant flux and attack the problem in a different and more general fashion than they did.

The analysis presented here, as applied to reverse osmosis, includes the special cases of flow inside tubes, outside tubes, between parallel plates, and in annuli. To reduce the number of parameters necessary to describe the problem it is assumed the flow is fully developed when the membrane section is approached. This analysis deals with the nonlinear brine side diffusion problem, and, as in previous work (*2* to *4, 6, 8*), it is assumed that Equation (4) relates the water flux to the pressure drop across the membrane.

ANALYSIS

Figure 1 shows the coordinate system used, and for a constant fluid property system the continuity, momentum, and diffusion equations can be written as

$$\frac{\partial u}{\partial x} + \frac{1}{r}\frac{\partial}{\partial r} rv = 0 \tag{1}$$

$$u\frac{\partial u}{\partial x} + v\frac{\partial u}{\partial r} = -\frac{1}{\rho}\frac{\partial P}{\partial x} + \nu\frac{1}{r}\frac{\partial}{\partial r} r\frac{\partial u}{\partial r} \tag{2}$$

$$u\frac{\partial w_s}{\partial x} + v\frac{\partial w_s}{\partial r} = \frac{D}{r}\frac{\partial}{\partial r} r\frac{\partial w_s}{\partial r} \tag{3}$$

Flow through the membrane is described by

$$|v_w| = A\,[\Delta P - \pi_o\,\theta(x, R_k)] = A\Delta P\,[1 - B_2\,\theta(x, R_k)] \tag{4}$$

where $k = 1, 2$ and v_w will be negative and positive at the lower and upper walls, respectively. The mass flux of salt in the r direction is given by

$$n_s = w_s \rho v - \rho D \frac{\partial w_s}{\partial r} \tag{5}$$

but for an ideal membrane the salt flux vanishes at the wall so that Equation (5) yields

$$D\frac{\partial w_s}{\partial r}(x, R_k) = v_w\, w_s(x, R_k) \tag{6}$$

The following mathematical analysis will be based upon consideration of the lower wall (that is, $r = R_1$ in Figure 1). The treatment of the upper wall is very similar, so only the results will be given in that case.

Since primary concern is with the region near the wall, we define a new transverse coordinate

$$y_1 = r - R_1 \tag{7}$$

Equations (1) and (3) then become, respectively

$$\frac{\partial u}{\partial x} + \frac{1}{y_1 + R_1}\frac{\partial}{\partial y_1}(y_1 + R_1)\,v = 0 \tag{8}$$

$$u\frac{\partial w_s}{\partial x} + v\frac{\partial w_s}{\partial y_1} = \frac{D}{y_1 + R_1}\frac{\partial}{\partial y_1}(y_1 + R_1)\frac{\partial w_s}{\partial y_1} \tag{9}$$

If u is expanded in a Taylor series as

$$u = \sum_{i=1}^{\infty} \frac{1}{i!}\left.\frac{\partial^i u}{\partial y_1{}^i}\right|_0 y_1{}^i \tag{10}$$

since $u(x, 0)$ is zero, then Equation (8) may be integrated to get

$$v = \frac{R_1}{y_1 + R_1} v_{w1} - \frac{1}{y_1 + R_1}\sum_{i=1}^{\infty}\frac{1}{i!}\frac{\partial}{\partial x}\left(\left.\frac{\partial^i u}{\partial y_1{}^i}\right|_0\right)\left[\frac{y_1{}^{i+2}}{i+2} + \frac{R_1 y_1{}^{i+1}}{i+1}\right] \tag{11}$$

and Equation (9) becomes

$$\sum_{i=1}^{\infty}\frac{1}{i!}\left.\frac{\partial^i u}{\partial y_1{}^i}\right|_0 y_1{}^i\frac{\partial w_s}{\partial x} + \left\{\frac{R_1 v_{w1}}{y_1 + R_1} - \frac{1}{y_1 + R_1}\sum_{i=1}^{\infty}\frac{1}{i!}\frac{\partial}{\partial x}\left(\left.\frac{\partial^i u}{\partial y_1{}^i}\right|_0\right)\left[\frac{y_1{}^{i+2}}{i+2} + \frac{R_1 y_1{}^{i+1}}{i+1}\right]\right\}\frac{\partial w_s}{\partial y_1} = \frac{D}{y_1 + R_1}\frac{\partial}{\partial y_1}(y_1 + R_1)\frac{\partial w_s}{\partial y_1} \tag{12}$$

Since in the brine system being considered the Schmidt number is approximately 560, mass transfer will be restricted to an extremely thin region compared with momentum transfer. Therefore we may, to a good approximation, retain in Equation (10) only the first two terms of the Taylor series for u so that

$$u \cong \left.\frac{\partial u}{\partial y_1}\right|_0 y_1 = \frac{\tau_{w1}}{\mu} y_1 \tag{13}$$

Furthermore, from Equation (11) it is clear that for very small y_1

$$v \cong \frac{R_1}{y_1 + R_1} v_{w1} \tag{14}$$

Estimates of the error involved in approximating v in a similar manner for a parallel plate system are given in reference 3. The error was found to be reasonably small,

especially if the interfacial mass transfer begins with an initially fully developed velocity field. It is easy to see that Equation (14) follows exactly from Equation (11) if the flow is fully developed and $v_w \cong 0$, which corresponds to $(d\tau_w/dx) = 0$. For illustrative purposes a reasonable value of v_w/u_b is, say, 5×10^{-5} in which case τ_w is constant within 5% for 1,000 radii downstream of the membrane leading edge.

If one uses the above approximations, which are very accurate for small x, along with Equation (4), and defines the new variables

$$\eta = \frac{A\Delta P y_1}{D}, \quad \lambda = \frac{(A\Delta P)^3 \mu}{D^2} \int_0^x \frac{dx}{\tau_{w1}},$$

$$\theta = \frac{w_s}{w_s(0,\eta)}, \quad \eta_1 = \frac{A\Delta P R_1}{D}$$

Equation (12) becomes

$$\eta \frac{\partial\theta}{\partial\lambda} - \frac{\eta_1}{\eta+\eta_1}[1 - B_2\theta(\lambda,0)]\frac{\partial\theta}{\partial\eta} = \frac{1}{\eta+\eta_1}\frac{\partial}{\partial\eta}(\eta+\eta_1)\frac{\partial\theta}{\partial\eta} \qquad (15)$$

which obviously reduces to the form of the parallel plate case as $\eta_1 \to \infty$. With the further transformations

$$\sigma = (9\lambda)^{1/3}, \quad \beta = \eta(9\lambda)^{-1/3}$$

Equation (15) becomes

$$\frac{\partial^2\theta}{\partial\beta^2} - 3\beta\sigma\frac{\partial\theta}{\partial\sigma} + 3\beta^2\frac{\partial\theta}{\partial\beta} = -\sigma[1 - B_2\theta(\sigma,0)]\frac{\partial\theta}{\partial\beta} + \eta_1^{-1}\sigma\left[-\beta\left(\frac{\partial^2\theta}{\partial\beta^2} + 3\beta^2\frac{\partial\theta}{\partial\beta} - 3\beta\sigma\frac{\partial\theta}{\partial\sigma}\right) - \frac{\partial\theta}{\partial\beta}\right] \qquad (16)$$

Equation (16) describes the inner tube of an annulus, and the parameter η_1 is a measure of the transverse curvature of the tube. Clearly, for large η_1 the curvature is small and vice versa.

Since interest is primarily in the entrance region, it is reasonable to expand θ in a Taylor series in σ as

$$\theta = 1 + \sum_{i=1}^{\infty} \theta_i(\beta)\,\sigma^i \qquad (17)$$

If Equation (17) is inserted into Equation (16), one obtains an infinite set of ordinary differential equations of the general form

$$\theta''_i + 3\beta^2\theta'_i - 3\beta i\,\theta_i = -\theta'_{i-1} + B_2\sum_{j=0}^{i-1}\theta_j(0)\theta'_{i-j-1} + \eta_1^{-1}g_i$$

$$g_i = -\left[\beta\left\{-\theta'_{i-2} + B_2\sum_{j=0}^{i-2}\theta_j(0)\,\theta'_{i-j-2} + \eta_1^{-1}g_{i-1}\right\} + \theta'_{i-1}\right] \qquad (18)$$

wherein $g_o = g_1 = 0$.

The same procedure may be followed for the upper wall, with the transformations

$$y_2 = R_2 - r$$

$$\lambda = \frac{(A\Delta P)^3\mu}{D^2}\int_0^x \frac{dx}{\tau_{w2}}$$

The final set of equations obtained is the same as for the lower wall except that $\eta = \dfrac{y_2 A\Delta P}{D}$, and η_1^{-1} is replaced by $-(\eta_2)^{-1} = -\left(\dfrac{R_2 A\Delta P}{D}\right)^{-1}$, so that Equation (16) is replaced by

$$\frac{\partial^2\theta}{\partial\beta^2} - 3\sigma\beta\frac{\partial\theta}{\partial\sigma} + 3\beta^2\frac{\partial\theta}{\partial\beta} = -\sigma[1 - B_2\theta(\sigma,0)]\frac{\partial\theta}{\partial\beta} - \eta_2^{-1}\sigma\left[-\beta\left(\frac{\partial^2\theta}{\partial\beta^2} + 3\beta^2\frac{\partial\theta}{\partial\beta} - 3\beta\sigma\frac{\partial\theta}{\partial\sigma}\right) - \frac{\partial\theta}{\partial\beta}\right] \qquad (19)$$

for the upper wall.

For both the upper and lower walls, the boundary conditions are

$$\theta(0,\infty) = 1 \qquad (20)$$

$$\frac{\partial\theta}{\partial\beta}(\sigma,\infty) = 0 \qquad (21)$$

$$-\frac{\partial\theta}{\partial\beta}(\sigma,0) = \sigma\theta(\sigma,0)\,[1 - B_2\,\theta(\sigma,0)] \qquad (22)$$

where Equation (22) follows directly from Equation (6). When one combines Equations (17), (20), (21), and (22) the boundary conditions are described by

$$\theta_i'(\infty) = 0 \qquad (23)$$

$$\left\{\begin{array}{l} -\theta_i'(0) = 1 - B_2 \\ -\theta_i'(0) = (1-2B_2)\,\theta_{i-1}(0) - B_2\sum_{j=1}^{i-2}\theta_j(0)\,\theta_{i-j-1}(0), \quad i \geq 2 \end{array}\right\} \qquad (24)$$

THE METHOD OF SOLUTION

By using Equation (17) the problem of solving Equations (16), (20), (21), and (22) is reduced to solving the linear set of Equations (18) and (24). Because of the linearity of the system one can use superposition to generalize the functions which must be determined numerically. It is seen that $\theta_0(\beta) = 1$ is necessarily what one would have obtained if $\theta_0(\beta)$ had been left arbitrary in Equation (17), rather than writing it as unity at the start.

From Equations (18), (23), and (24) with $i = 1$, one gets

$$\theta_1'' + 3\beta^2\theta_1' - 3\beta\theta_1 = 0$$

$$\theta_1'(\infty) = 0$$

$$-\theta_1'(0) = 1 - B_2$$

for which the exact solution is

$$\frac{\theta_1}{1-B_2} = \frac{e^{-\beta^3}}{\Gamma\left(\frac{2}{3}\right)} - \beta\left[1 - \frac{\Gamma\left(\frac{2}{3},\beta^3\right)}{\Gamma\left(\frac{2}{3}\right)}\right]$$

and $\Gamma\left(\dfrac{2}{3},\beta^3\right)$ is the incomplete gamma function. The differential equation and boundary conditions for θ_2 are

$$\theta_2'' + 3\beta^2\theta_2' - 6\beta\theta_2 = (B_2 - 1)\,\theta_1' + \eta_K^{-1}(-\theta_1')$$

$$\theta_2'(\infty) = 0$$

$$-\theta_2'(0) = (1 - 2B_2)\theta_1(0)$$

where η_K denotes both η_1 and η_2. Thus, let

$$\theta_2 = \phi_{21} + \eta_K^{-1}\phi_{22}$$

and by equating coefficients of η_K^{-1} the results are

$$\phi_{21}'' + 3\beta^2\phi_{21}' - 6\beta\phi_{21} = (B_2 - 1)\theta_1'$$

$$\phi_{21}'(\infty) = 0$$

$$-\phi_{21}'(0) = (1 - 2B_2)\,\theta_1(0)$$

$$\phi_{22}'' + 3\beta^2\phi_{22}' - 6\beta\phi_{22} = -\theta_1'$$

$$\phi'_{22}(\infty) = 0$$

$$\phi_{22}'(0) = 0$$

When $i = 3$, one can take

$$\theta_3 = \phi_{31} + \eta_K^{-1}\phi_{32} + \eta_K^{-2}\phi_{33}$$

to get

$$\phi_{31}'' + 3\beta^2\phi_{31}' - 9\beta\phi_{31} = (B_2 - 1)\,\phi_{21}' + B_2\,\theta_1(0)\,\theta_1'$$

$$\phi_{31}'(\infty) = 0$$

$$-\phi_{31}'(0) = (1 - 2B_2)\,\phi_{21}(0) - \theta_1^2(0)\,B_2$$

$$\phi_{32}'' + 3\beta^2\phi_{32}' - 9\beta\phi_{32} = (B_2 - 1)\phi_{22}' + (1 - B_2)\beta\theta_1' - \phi_{21}'$$

$$\phi_{32}'(\infty) = 0$$

$$-\phi_{32}'(0) = (1 - 2B_2)\,\phi_{22}(0)$$

$$\phi_{33}'' + 3\beta^2\phi_{33}' - 9\beta\phi_{33} = \beta\theta_1' - \phi_{22}'$$

$$\phi_{33}'(\infty) = 0$$

$$\phi_{33}'(0) = 0$$

etc.

Exactly the same procedure is followed for θ_i, $i > 3$. Furthermore, the solutions can be generalized further by employing a similar approach with respect to B_2. However, the number of functions involved becomes large rapidly, and therefore only a few selected specific values of B_2 were used in this work since these were considered to be sufficient to determine the general trend of results for annuli.

The salt concentration at the surface is of primary interest since it fixes the magnitude of the flux v_w, as given in Equation (4). Clearly, $\theta(x, 0)$ is known once the $\theta_i(0)$ have been determined. Also the $\theta_i(0)$ are in turn fixed once the ϕ_{ij}, $j \leq i$, have been determined. For $B_2 = 0.25$ these results are given as

$$\left.\begin{aligned}
\theta_1(0) &= 0.55387\\
\theta_2(0) &= 0.045093 - 0.18074\,\eta_K^{-1}\\
\theta_3(0) &= -0.03262 - 0.058053\,\eta_K^{-1} + 0.63308\,(\eta_K^{-1})^2\\
\theta_4(0) &= -0.0029264 + 0.0262275\,\eta_K^{-1} + 0.025612\,(\eta_K^{-1})^2 - 0.0033953\,(\eta_K^{-1})^3\\
\theta_5(0) &= 0.0030747 + 0.0093497\,(\eta_K^{-1}) - 0.0096629\,(\eta_K^{-1})^2 - 0.006176\,(\eta_K^{-1})^3 + 0.00012719\,(\eta_K^{-1})^4
\end{aligned}\right\} \quad (25)$$

where η_K denotes the magnitude of the parameter at the lower wall when $K = 1$ and at the upper wall when $K = 2$. Furthermore, η_K is positive for η_1 and negative for η_2.

RESULTS AND DISCUSSION

Inspection of Equations (15) and (19) reveals immediately that they are identical in form to the parallel plate case for large η_K, or as the Peclet number based on wall velocity gets large. In this event, the diffusional behavior at each wall is different only to the extent that the shear stresses at each wall differ.

This is the case for which the asymptotic solution of Dresner (8), for $B_2 = 0$, applies equally well to both parallel plates and tubes.* As one might expect, as transverse curvature increases, or $\eta_K \to 0$, then the analogy suggested in references 8 and 9 does not apply well even very close to the inlet as can be seen in Figure 2. However, on the basis of Figure 4 in reference 8 it seems that this is not a very serious practical limitation.

The results of most practical interest are, of course, related to the water produced per unit time per unit width of a single membrane for a given set of operating conditions. This quantity is given by

$$Q = \int_o^x |v_w|\,dx \qquad (26)$$

If the wall shear stresses τ_{wK} are constant, as they are assumed to be in the fully developed flows considered here, then Equation (26) can be written in dimensionless form as

$$Q^+ = \frac{Q(A\Delta P)^2 9\mu}{D^2\,\tau_{wK}} = \sigma^3\left[\,1 - 3\,B_2\sum_{i=0}^{\infty}\theta_i\,(0)\,\frac{\sigma^i}{i+3}\,\right]$$

A convenient quantity to aid in visualizing the effect of concentration polarization is the ratio of the fraction of feed converted to pure water to the fraction that would be converted if the transverse velocity at the wall remained equal to $v_w(0)$. This quantity will be called the efficiency E, which is given by

$$E = Q/v_w(0)x$$

The preceding quantities can be calculated very easily once the $\theta_i(0)$ are known. For $B_2 = 0.25$, general expres-

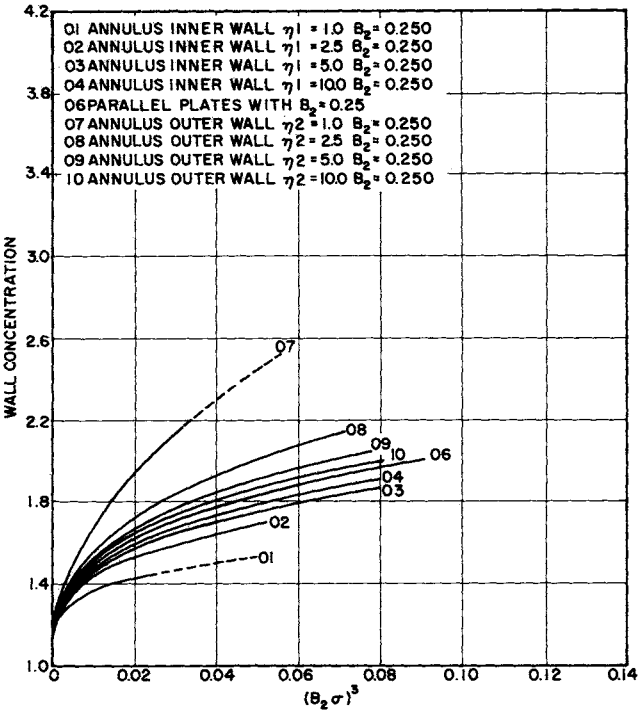

Fig. 2. Effect of parameters η_1 and η_2 on wall concentration distribution for $B_2 = 0.25$.

* Note that $\alpha = \eta_K^{-1}$ if $B_2 = 0$. Thus, on the basis of reference 8, it is seen that the importance of α is determined by downstream distance in rectilinear systems and by both this and transverse curvature in curvilinear systems.

TABLE 1. VALUES OF $\theta_i(0)$

B_2	η_K	$\theta_1(0)$	$\theta_2(0)$	$\theta_3(0)$	$\theta_4(0)$	$\theta_5(0)$
0	1	0.738488	—0.000327	—0.001308	—0.0000474	0.00001569
0	10	0.738488	0.2166	0.03039	0.0017029	—0.00003598
0	∞	0.738488	0.2407	0.04384	0.004446	0.0001591
0	—1	0.738488	0.4817	0.2868	0.1588	0.08289
0	—10	0.738488	0.2648	0.0592	0.00867	0.000741
0.125	1	0.6462	—0.0793	—0.002987	0.00489	—0.001411
0.125	10	0.6462	0.1105	—0.1767	—0.00681	0.0007262
0.125	∞	0.6462	0.1316	—0.01064	—0.008340	—0.0001309
0.125	—10	0.6462	0.1527	—0.001896	—0.009044	—0.001171
0.125	—1	0.6462	0.3425	0.1548	0.06058	0.02076
0.25	1	0.55387	—0.13565	0.01455	0.00731	—0.00516
0.25	2.5	0.55387	—0.027203	—0.031576	0.009153	0.000971
0.25	5.0	0.55387	0.00894	—0.03506	0.00336	0.0028
0.25	∞	0.55387	0.04509	—0.03261	—0.002926	0.003075
0.25	—1	0.55387	0.22583	0.06883	0.015125	0.00283
0.25	—2.5	0.55387	0.11739	—0.00987	—0.01048	—0.000694
0.25	—5.0	0.55387	0.08124	—0.02421	—0.00808	0.00169
0.5	1	0.3692	—0.18077	0.06915	—0.014103	—0.005352
0.5	10	0.3692	—0.07231	—0.01197	0.01297	—0.002713
0.5	∞	0.3692	—0.06028	—0.01603	0.01165	—0.001262
0.5	—10	0.3692	—0.04821	—0.01912	0.009945	—0.000023
0.5	—1	0.3692	0.06026	—0.002305	0.0002282	0.002926

Positive values of η_K denote η_1 and negative values denote η_2.

sions for any value of η_K are given by Equations (25) for the first five $\theta_i(0)$. Additional data, for $B_2 = 0$, 0.125 and 0.5, are given in Table 1.

The variable σ, for constant shear stress systems, is defined as

$$\sigma = A\Delta P\left[\frac{9\mu}{D^2\tau_{wK}}x\right]^{1/3} \tag{27}$$

where τ_{wK}, $K = 1,2$, denotes the shear stress at the lower and upper walls. From an experimental point of view, the quantities u, π_o, and x are the easiest to vary, and also one can visualize a linear dependence on x most easily. Therefore, since $\pi_o = B_2\Delta P$, the results in Figures 2, 3, and 4 were plotted in terms of $(B_2\sigma)^3$.

In Figure 2, one can see that the effect of the parameters η_K is to decrease concentration polarization at the inner wall and increase it at the outer wall. The designation parallel plates for curve 6 is merely meant to denote that the form of Equations (16) and (19) is identical to the parallel plate case. Actually, this case simply corresponds to $\eta_K = \infty$.

In viewing Figure 2, it should be remembered that the form of τ_{wK} depends on the system under consideration. For example, if one is interested in a tube, then attention should be directed to the outer wall. Furthermore, if $\eta_2 = \infty$, then the parallel plate form applies. However, for tubes $\tau_{w2} = (4\,u_b\mu/R_2)$, in contrast to parallel plates for which $\tau_{w2} = (3\,u_b\,\mu/R_2)$. Thus for a given $[v_w(0)/u_b]$ (x/R_2), one would find significantly lower polarization for tubes than plates. Clearly, as seen on Figure 2, this reduction is modified for finite η_2. Wall concentration distribution results for systems with other values of B_2 are similar to those shown.

In judging the effect of the η_K, it should be remembered that

$$\eta_K = \frac{A\Delta PR_k}{D} = \frac{v_w(0)R_k}{(1-B_2)D}$$

so that for a throughput of 40 gal. of water/(sq.ft.)(day) $\simeq 18.8 \times 10^{-4}$ cm./sec. and $D = 1.6 \times 10^{-5}$ sq.cm./sec.

$$\eta_K \cong 117\frac{R_k}{1-B_2}$$

whereas if the throughput is 10 gal./(sq.ft.)(day)

$$\eta_K \cong 29\frac{R_k}{1-B_2},\ R_k \text{ in cm.}$$

Consequently, values of η_K on the order of unity are not unreasonable for small diameter capillaries.

Figure 3 shows how $B_2^2Q^+$ varies with $(B_2\sigma)^3$. The quantity $B_2^2Q^+$ was employed since it is defined in terms of π_o rather than ΔP. This figure, as well as Figure 4, shows that Q^+ and E, which are obtained by integration, are much less sensitive to radii variations than is the wall concentration distribution. However, the changes in wall concentration will be reflected in Q^+ and E further downstream.

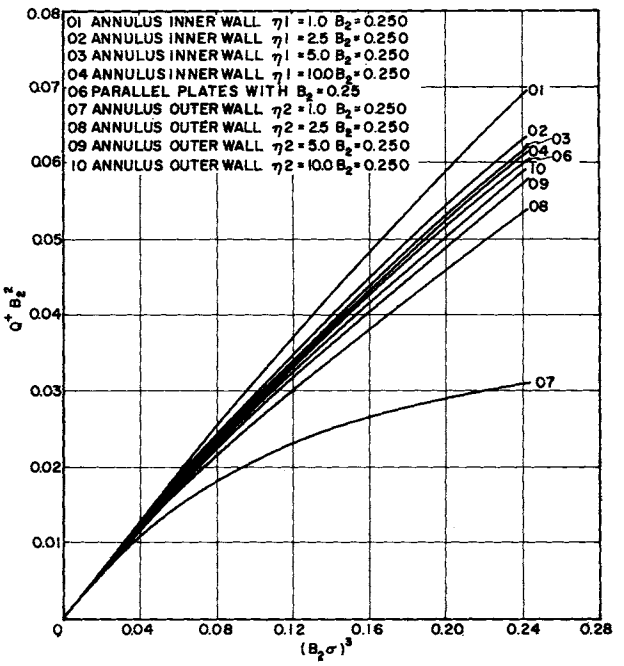

Fig. 3. Effect of parameters η_1 and η_2 on productive capacity of membrane for $B_2 = 0.25$.

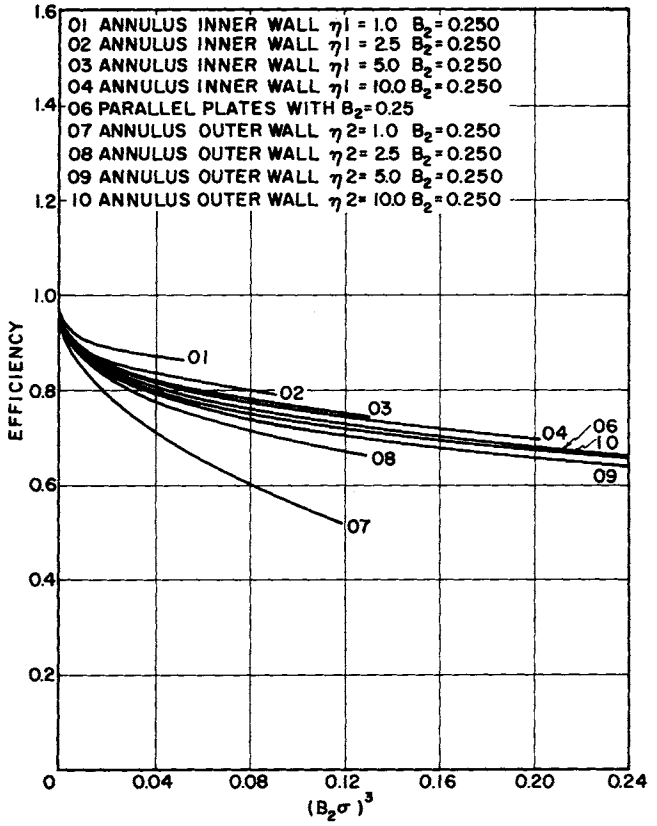

Fig. 4. Effect of parameters η_1 and η_2 on efficiency for $B_2 = 0.25$.

Results of the present analysis have been compared with the experimental data of Merten, Lonsdale, and Riley (6), who used a parallel plate system and reported throughput data as a function of bulk velocity. It was found that the fully developed laminar flow theory agreed quite well with their experimental results. The percentage error was about 5, which is probably within experimental error (4).

PROCEDURE FOR APPLYING RESULTS

To use the preceding results one would proceed in the following fashion:

Once the hydrostatic pressure drop across the membrane and the feed brine concentration, which fixes the osmotic pressure at $x = 0$, are specified, the value of B_2 is known. For given membrane constant A and annulus radii R_k the parameters η_k are fixed once the brine diffusion coefficient is stipulated. The shear stresses τ_{wk} at the inner wall $k = 1$ and the outer wall $k = 2$ are known once the Reynolds number and the ratio of the radii are chosen, and these τ_{wk} relate x, the linear distance along the wall, to the dimensionless coordinate σ by Equation (27).

Once B_2 and η_k are known, the $\theta_i(0)$ can be read from Table 1. Then, the $\theta_i(0)$ can be used in Equation (17) to determine the wall concentration distribution, as a function of x, which in turn is used in Equation (4) to determine the flux distribution along the conduit. Then Equation (26), or Q^+, can be used to determine the rate of production of water by the system.

ACKNOWLEDGMENT

This work was supported by the Office of Saline Water of the U. S. Department of the Interior under grant number 14-01-0001-664.

NOTATION

A = membrane constant as defined in Equation (4)
B_2 = $\pi_o/\Delta P$
D = diffusion coefficient
E = fraction of feed converted to fresh water divided by the fraction that would be converted if the wall velocity were $v_w(0)$ along the entire conduit
n_s = mass flux of salt as defined in Equation (5)
ΔP = total pressure drop across membrane
Q = volume of water produced per unit time per unit width of membrane
r = defined in Figure 1
R_1 = radius of inner wall
R_2 = radius of outer wall
u = axial velocity
u_b = bulk velocity of brine at $x = 0$
v = transverse velocity
$v_w(0)$ = transverse velocity at wall at entrance to system
w_s = mass fraction of salt in brine
x = axial distance coordinate
y_i = transverse distance coordinates as defined in Figure 1

Greek Letters

α = $[D/v_w(0)\ R_2]$
β = $\eta\sigma^{-1}$
η = dimensionless coordinate, $y_i(A\Delta P/D)$
θ = dimensionless mass fraction, $w_s/w_s(0, \eta)$
λ = $\dfrac{(A\,\Delta P)^3\,\mu}{D^2}\displaystyle\int_o^x \frac{dx}{\tau_w(x)}$
μ = viscosity
ν = kinematic viscosity
π = osmotic pressure of a saline solution
π_o = osmotic pressure at $x = 0$
ρ = density
σ = $(9\lambda)^{1/3}$
τ_w = shear stress at membrane wall

Subscripts

b = bulk value
w = value at membrane surface
k = 1 denotes lower wall and 2 denotes upper wall
s = salt component

LITERATURE CITED

1. Bretton, E. J., *O.S.W. Res. Develop. Progr. Rept. No. 16* (Apr., 1957).
2. Gill, W. N., Chi Tien, and D. W. Zeh, *Ind. Eng. Chem. Fundamentals*, **4**, 433 (1965).
3. ———, Quart. Rept., Jan. 1, 1965-March 31, 1965. Contract 14-01-0001-401, Office Saline Water, U. S. Dept. Interior; *Intern. J. Heat Mass Transfer*, **9**, 907 (1966).
4. ———, *Ind. Eng. Chem. Fundamentals*, **5**, 367 (1966).
5. Loeb, S., and S. Sourirajan, *U.C.L.A. Dept. Eng. Rept. No. 60-60* (1960).
6. Merten, Ulrich, H. K. Lonsdale, and R. L. Riley, *Ind. Eng. Chem. Fundamentals*, **3**, 210 (1964).
7. Michaels, A. S., H. J. Bixler, and R. M. Hodges, *J. Colloid Sci.*, **20**, 1034 (1965).
8. Sherwood, T. K., P. L. T. Brian, R. E. Fisher, and Lawrence Dresner, *Ind. Eng. Chem. Fundamentals*, **4**, 113 (1965).
9. Fisher, R. E., T. K. Sherwood, and P. L. T. Brian, *Office Saline Water, Res. Develop. Progr. Rept. No. 141* (Sept., 1965).
10. *Chem. Eng.*, **71**, 81 (May 11, 1964).
11. Mahon, H. I., *Natl. Acad. Sci. Publ. 942*, 345 (1963).

Manuscript received October 25, 1965; revision received May 2, 1966; paper accepted May 4, 1966. Paper presented at A.I.Ch.E. Philadelphia meeting.